ISSN (Print) 1226-1750
ISSN (Online) 2233-6656
Journal of Magnetics 22(2), 214-219 (2017) https://doi.org/10.4283/JMAG.2017.22.2.214

Magnetic Particle Separation by an Optimized Coil: A Graphical User Interface

Kasra Rouhi, Amirhossein Hajiaghajani, and Ali Abdolali*

Applied Electromagnetics Lab, School of Electrical Engineering, Iran University of Science and Technology, Tehran 1684613114, Iran

(Received 1 January 2017, Received in final form 6 April 2017, Accepted 28 April 2017)

Magnetic separators that clean the fluid stream from impurities, protect the installations in numerous industries. This paper introduces a graphical user interface (GUI) which proposes an optimized coil separating magnetic particles with a radius from 1 up to 500 μm. High gradient magnetic fields are employed in an arbitrary user defined fluidic channel which is made of a nonmetallic material. The effects of coil parameters are studied and adjusted to design an optimum coil with a minimum Ohmic loss. In addition, to design the coil scheme based on the particle movements, a mathematical particle-tracing model within the fluid channels has been utilized. In comparison to conventional magnetic separators, this model is reconfigurable by the user, produces a weaker magnetic field, allows for continuous purifying and is easy to install, with high separation efficiency. The presented GUI is simple to use, where the coil's manufacturing limitations can be specified.

Keywords : Magnetic separation, Graphical user interface (GUI), High gradient magnetic field, Multi turn Coil

1. Introduction

Magnetic particle separation refers to splitting magnetizable particles suspended in nonmagnetic fluid, employing external magnetic forces along a pipeline under separation. The general separation techniques have been broadly used for chemical and biological analysis [1-4]. The majority of particle separation methods employ centrifugal force, magnetophoresis (e.g. moving iron particles by a magnet) [5], dielectrophoresis (using electric charges of particles to move them) which is electric analogous of magnetophoresis [6], and also acoustophoresis [7]. The centrifugal force, the most common industrial method, is produced by spinning impure fluid in a rotating chamber. However, this approach is not applicable for a wide range of fluid transmission lines because of their large, complex or fragile structure. It is also unable to separate particles based on their magnetization.

The electrophoretic method is highly dependent on the material of which the pipeline is made; therefore, It is less applicable in industrial usages [8].

The magnetic based separation comes with numerous industrial advantages such as removal of dissolved heavy metals, filtration, and phosphate removal [9-11]. The method of magnetic separation has been used for several decades in various separating devices by inserting static or rotating magnets along with the fluid flow (see Fig. 1a&b). However, most of traditional magnet separation techniques such as magnet bars, require fluid flow interrupt for some minutes, to clean the magnets. This is a time consuming process and slows down the setup's operation. In addition, their separation rate will decrease while particles accumulate around the magnet bars.

Due to the recent efforts on developing and synthesis of super paramagnetic micro/nano particles and their undeniable biomedical applications such as magnetic cell separation [12] and steering of microbots inside the human body [13, 14], the magnetophoresis steering technique is broadly employed.

Here, we study the magnetic particle separation, where the coil is placed outside of the channel. Coil's specifications (see Fig. 1c) are discussed and the particles trace is considered. Impurities take an exit through an adjunct branch and accumulate in a chamber by a simple magnet.

Recent works pinpointed coil designs and structures to insure the magnetic particles move toward the region of interest. Nevertheless, there were two critical problems not addressed before: first, such structures must be placed through the fluid flow (they are called invasive methods,

*Corresponding author: Tel: +98-21-7322-5726
Fax: +98-21-7322-5777, e-mail: abdolali@iust.ac.ir

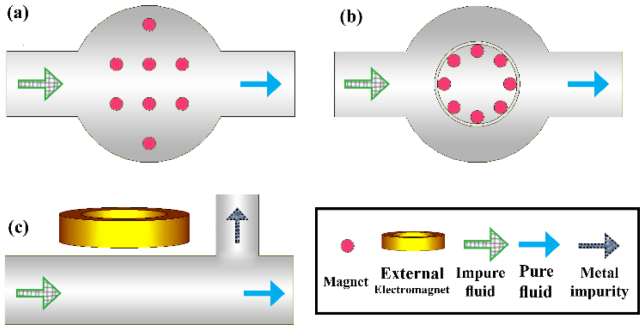

Fig. 1. (Color online) Conventional separator devices work by inserting (a) static or (b) rotating magnets along with the fluid flow. (c) Placing an external coil is easy to install and enables us to separate particles incessantly and without stopping the fluid flow for magnet cleaning.

which may deform the pipelines) where particles stick to the magnets and reduce the fluid flow. We aim to design a system that non-invasively separates the impurities. Second, most of those structures were not able to operate on large pipelines (with a cross section area larger than 3 cm^2) that are consisting of higher fluid velocity (greater than 10 cm/s). Traditional magnetic separators such as bar magnets and grate magnets produce a strong magnetic field of 0.3-1.5 T, which may affect other systems close to the magnet and need to be cleansed of impurities regularly. They are also highly weighted and must be kept at a controlled temperature.

In the studies focused on magnetic separation, developing an algorithm to design a high gradient magnetic field has not been addressed significantly. This can speed up the design procedure while minimizing the consumed power simultaneously. In this paper, we consider practical considerations and develop a Matlab-based GUI, based on the databank provided by finite element simulations of various coils. We propose a new geometry of ferromagnetic core to produce a high gradient magnetic field and lower the magnetic flow loss. The GUI gets the physical parameters of the pipeline, plus fluid-particle properties. As the output, a low power consuming coil design and particle trajectory graph would be proposed to insure the separation. The proposed setup is easy to install and costs much less than those strong permanent magnets. Also, it proposes reconfigurable properties and is developed based on industrial user needs.

2. Physics of Magnetic Particle Separation

We assume that impure fluid is piping inside a transmission line cylinder. Thereby, the drag force created by fluid flow dramatically affects particle trajectory. The scenario of separation is to form a magnetic force, which can change the particle trajectory and deliver them into a targeted exit branch. The worst case is where particles are targeted from the furthest part of the pipeline toward the nearest part (along the z-axis in our model). The involved forces are discussed in this section.

2.1. Magnetophoretic force

We consider a current carrying multiturn coil as the external actuator producing a magnetic field (H) which simultaneously magnetizes spherical ferromagnetic particles suspended in fluid and pull them toward the exit branch [15]. Particles get an effective magnetic moment under the action of given by [16]:

$$M_{eff} = 4\pi r_p^3 \left[\frac{\mu_p - \mu_f}{\mu_p + 2\mu_f} H + \frac{\mu_p}{\mu_p + 2\mu_f} M \right] \quad (1)$$

where μ_f, μ_p and r_p are respectively fluid permeability, particle permeability and spherical particle radius. Bold characters denote vector fields. If particles possess the linear magnetic permeability, it can be shown that magnetic moment is derived by:

$$M = \frac{\mu_f}{\mu_f - 1} H \quad (2)$$

Considering soft ferromagnetic particles, they exhibit nonlinear magnetic moment behavior and thus (1) can be reduced to form the magnetophoretic force [15]:

$$F_{MP} = 2\pi\mu_f r_p^3 \frac{\mu_p - \mu_f}{\mu_p + 2\mu_f} \nabla H^2 \quad (3)$$

Note that $\nabla H^2 = 2(H.\nabla)H$, hence, based on (3) we require an intense and high gradient magnetic field to increase the magnetic force.

2.2. Drag force

The hydrodynamic drag force is indicated by Stoke's law [17]:

$$F_D = 6\pi\eta r_p^3 (v_f - v_p) \quad (4)$$

where η, v_f, and v_p are respectively dynamic viscosity of fluid (fluid's resistance to sheering flows), fluid and particle velocity.

Magnetic separation is also affected by various forces such as gravity, buoyancy, and particle-particle interaction. However, many of those are often excluded from models due to negligible volume/surface ratio of particles with a diameter of 10-1000 μm [18]. The particle's path is obtained in subject to Newton's 2nd law of motion.

$$F_{MP} + F_D = m_p \frac{dv_p}{dt} \quad (5)$$

where $m_p(=\frac{4}{3}\pi r_p^3 \rho_p)$ is the spherical particle mass with the density of ρ_p. The analytic solution for z component movement is obtained by solving (5):

$$v_{p_z}(t) = v_{f_z} + \frac{F_{MP_z}}{6\pi\eta r_p} \times \left(1 - \exp\left(-\frac{6\pi\eta r_p}{m_p}t\right)\right) \quad (6)$$

We refer to the z component of a vector throughout this work by the index of z. To predict the particle trajectory, this equation is numerically solved by MATLAB ODE toolbox and is available in the proposed interface. Note that v_p is a function of time and thus leads to the accelerated movement.

3. Coil Optimization Factor

The simplified hydrodynamic model was explained. Here, we discuss the design parameters of the coil based on the particle trajectory.

According to (6), the exponential term is ignorable, since $6\pi\eta r_p/m_p$ is extremely large. Thereby, the particle movement in z direction can be approximated by a constant axial velocity motion of $v_f = F_{MP_z}/6\pi\eta r_p$. Note that $v_{f_z} = 0$, because of zero fluid velocity in non-axial direction. The time taken for particles to move along the z axis from the lowest part of the pipeline toward the highest part is obtained by:

$$\Delta t = \frac{p}{\frac{F_{MP_z}}{6\pi\eta r_p}} \quad (7)$$

Where p represents the pipe inner diameter (see Fig. 2). Besides, it takes particles Δt seconds to move along the accessible region of pipe (L, in x direction) which is equivalent to L/v_f because of constant velocity of fluid in the x-axis. Accordingly, (7) results in a formula by which the required magnetic force is obtained:

$$F_{MP_z} = 6\pi p v_f \eta r_p / L \quad (8)$$

This scalar parameter is utilized to compare different pipelines. By integrating F_{MP_z} over the accessible length, we obtain the integrated force:

$$F_{I_z} = \int_{-L/2}^{L/2} F_{MP_z}(z)dx \cong 6\pi p v_f \eta r_p . \quad (9)$$

The coil must be placed within the accessible region, nevertheless, if there is another outlet before the impurities chamber, particles move toward the undesirable outlet. In addition, circular coils produce most of the magnetic field beneath their loop. Hence, in our proposed setup, center of the coil is placed b+1 cm before the targeted exit branch (where b is the outer radius, which is clearly smaller than $L/2$). It should be noted that if the coil is placed farther from the exit branch, particle stick to the pipe walls; and if the coil is placed closer, particles cannot reach the highest part in the accessible region. Differential radius (d), coil height (h) and wire diameter (w) are simultaneously swept in order to reach the highest produced magnetophoretic force.

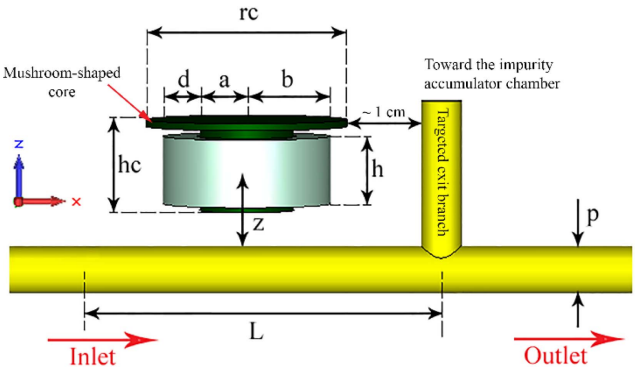

Fig. 2. (Color online) General model of separation channel and the non-invasive actuator system.

In this model, in order to simulate the real situation, the coil is made out by shielded copper wire and fed by voltage source, where the current and number of the turns can be calculated from total resistivity and coil dimensions, respectively. It should be noted that the wire length depends on the coil dimensions and is calculated from:

$$l_w = 2\pi \times \left(a + (a+w) + (a+2w) + \cdots + \left(a + \left\lfloor \frac{d}{w} \right\rfloor \times w\right)\right) \times \left\lfloor \frac{h}{w} \right\rfloor \quad (10)$$

where a is the coil inner radius. Therefore, the coil's resistance is calculated by:

$$R_{coil} = \frac{1}{\sigma_{\mathrm{Cu}}} \times \frac{l_w}{0.25\pi w^2} \quad (11)$$

where σ_{cu} is the copper conductivity. The required applied voltage can be simply found by Ohm's law.

The distance between the magnetic source and the pipeline (z_{min}) is a challenging issue for non-invasive magnetic separation, since it weakens the intensity of magnetic fields. Based on the analytic solution for the magnetic field [19], the intensity of produced magnetic fields is controlled by the applied voltage and is independent from the coil's geometrical parameters. The correspondence between the magnetic force versus the depth is considered in the interface.

To avoid wasting magnetic flow and create a high gradient magnetic field in the accessible region we em-

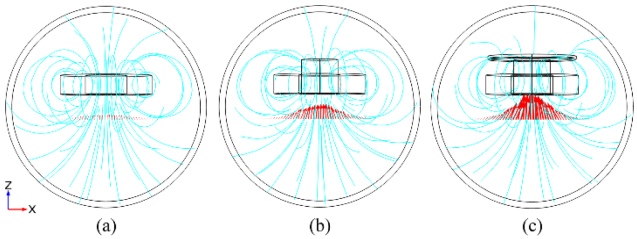

Fig. 3. (Color online) The comparison between magnetic forces enhanced by a: coil only, b: cylindrical core, c: mushroom-shaped core. Same coils running same currents are employed. Arrows depicted in the same scales represent the magnetic force along the pipeline placed 2 cm beneath the coil. Stream lines show the effects of cores.

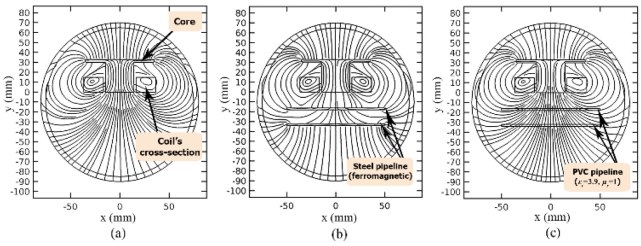

Fig. 5. (Color online) Due to the electromagnetic boundary conditions, the ferromagnetic pipeline affects magnetic fields. Magnetic fields a: without the presence of pipeline. b: where a ferromagnetic pipeline induces electromagnetic boundary conditions. c: do not change by a nonmagnetic pipeline.

ployed a ferromagnetic core made out of the widespread stainless steel ST-37. Three cases are compared: no core, cylindrical core, and cylindrical core on which a disc placed above (mushroom-shaped core). The nonlinear magnetization profile of the cores is considered in the simulation [20]. The efficiency of the mushroom-shaped core is shown in Fig. 3.

All simulations are repeated for different core shapes and mentioned in the GUI in where the user can select the best dimension and decide.

We have employed COMSOL's AC/DC stationary solver to retrieve the F_{lz} for all combinations of coil parameters. Fig. 4 represents the produced F_{lz} for different coil's structures. For a specific pipeline geometry, a unique

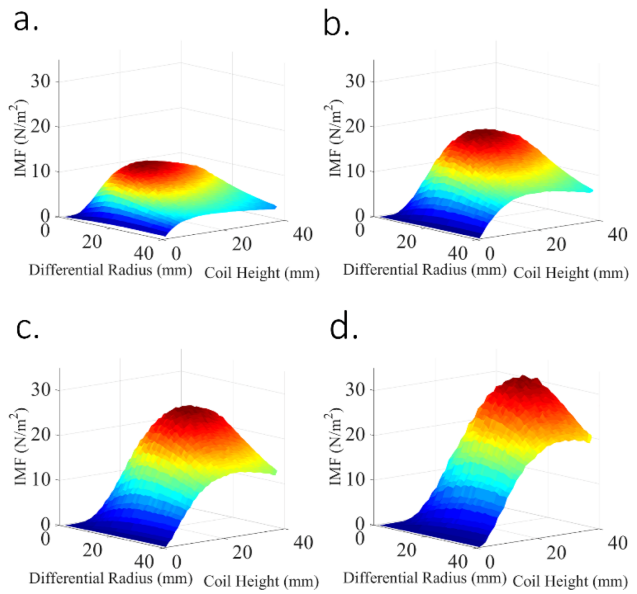

Fig. 4. (Color online) The optimization of integrated magnetic force (IMF) produced by different wire diameters (w). a: w=0.4, b: w=0.5, c: w=0.6, d: w=0.7 mm. The optimum coil parameters would be used for the user defined situation. Additional wire diameters are included in the GUI.

set of coil parameters results in the highest F_{lz} which would be picked up by the interface automatically.

The magnetic field must penetrate inside the pipeline; therefore, the pipeline must be made of non-magnetic material such as PVC, etc. To this end, a comparison between magnetic fields' pattern in pipelines made of magnetic and non-magnetic is drawn. It is observed that magnetic fields change in ferromagnetic pipelines due to the electromagnetic boundary condition (see Fig. 5).

The GUI's goal is to calculate and select the best parameter set in order to achieve the maximum particle

Table 1. GUI Input Parameters.

Parameters	Unit	Description
L	mm	Available region of coil placement
W	mm	Wire diameter (optional)
Q	L/min	Fluid flow rate
ρ_p	kg/m^3	Particle density
r_p	μm	Particle radius
p	mm	Pipe diameter
z_{min}	mm	Minimum distance between the coil and the pipe
Core	Yes/No	Based on finite element simulations, an appropriate core is considered (optional)

Table 2. GUI Output Parameters.

Parameters	Unit	Description
D	mm	Differential radius
H	mm	Coil's height
w	mm	Wire diameter
h_c	mm	Ferromagnetic core's height
ρ_c	mm	Cap's radius
A	mm	Coil's inner radius
Force	N/m^2	Produced F_{lz}
z	mm	Distance between the coil and the pipe
v_s	v	Voltage supply

(a)

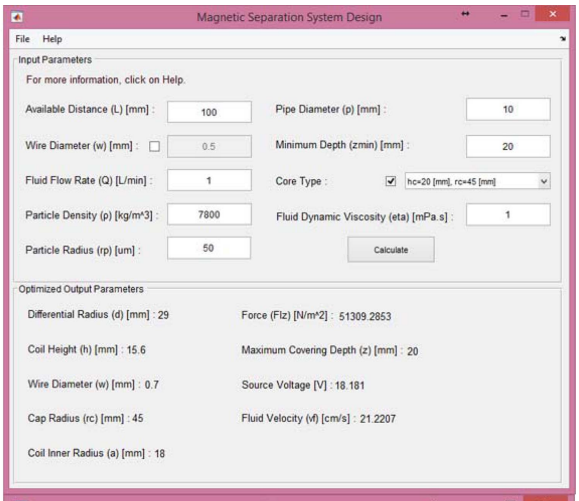

(b)

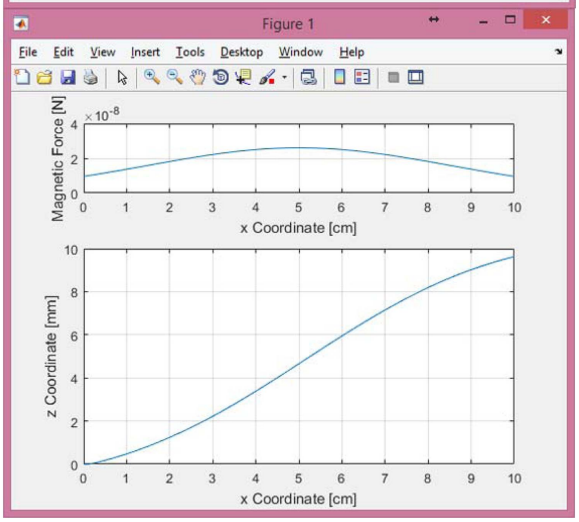

Fig. 6. (Color online) Designed graphical user interface; (a) Firstly, user must initialize the interface to add simulation data, following by filling the input parameters; (b) Particle dynamic is solved and the spatial form of applied force id depicted. Also, user can find how much it takes for particles to be delivered toward the exit branch.

guidance rate while using the minimum voltage supply. The user is required to enter all input parameters described in Table 1. This is to find the required force for successful separation. If the user does not apply a constraint on wire diameter, the GUI will suggest the best wire diameter to reach the highest available F_{Iz} while minimizing the voltage supply.

The GUI output consists of the spatial form of applied magnetophoresis and particle tracing under the optimized coil. This is to ensure that particles are moving toward the exit branch. Output parameters of the GUI are represented in Table 2.

4. A Practical Example

An example of a magnetic separation is where small iron particles with the density of 7.8 g/cm^3 and the radius of 50 μm float inside fluid passing through a PVC pipeline with the inner diameter of 4 mm, containing the flow rate of 1 L/min. The pipe centerline is placed 20 mm beneath the coil. The core employment is optional. First, the user enters the pipeline parameters.

Tables including magnetic forces values based on various parameter sets (whose data was shown in Fig. 4) are stored in the MS Excel files and located in the GUI's directory. In order to prevent overheating, a minimum voltage must supply the coil. The code selects the best combination of parameters. By pressing the calculate command, the interface proposes a coil design and then solves the dynamic equation under the user-defined condition. The interface and results of this example are shown in Fig. 6.

5. Conclusion

A responsive user interface is established to design a single current-carrying coil to change the trajectory of magnetic particles suspended in fluid flowing in a pipeline. The design algorithm is based on the user defined parameters for getting the geometric parameters of the low power consuming coil. Particles suspended in a laminar flow are separated based on their radius, density and magnetic permeability while the user specifies the minimum size of caught particle. In this interface, the trajectory of user defined particles is solved and based on their trajectory path, the best magnetic actuator would be selected among the pre-simulated coils. This GUI shows enormous practical potentialities in industrial magnetic separation, as it is easy to install, consumes much less power compared to conventional methods, costs much less and adjustable with the user needs while filtering metal objects out inside a pipeline. It also plays a didactic role for better understanding of particle dynamics within a fluid.

References

[1] C. W. Yung, J. Fiering, A. J. Mueller, and D. E. Ingber, Lab on a Chip **9**, 1171 (2009).
[2] O. Lara, X. Tong, M. Zborowski, and J. J. Chalmers, Exp. Hematol. **32**, 891 (2004).
[3] Y. H. Jang, M. J. Hancock, S. B. Kim, S. Selimović, W.

Y. Sim, H. Bae, and A. Khademhosseini, Lab on a Chip **11**, 3277 (2011).
[4] P. O. Krutzik, J. M. Crane, M. R. Clutter, and G. P. Nolan, Nat. Chem. Biol. **4**, 132 (2008).
[5] J. Oberteuffer, IEEE Trans. Magn. **10**, 223 (1974).
[6] H. A. Pohl, Cambridge Univ. Press, Cambridge (1978) pp. 232-254.
[7] F. Petersson, A. Nilsson, C. Holm, H. Jonsson, and T. Laurell, Analyst **129**, 938 (2004).
[8] P. R. C. Gascoyne and Jody Vykoukal, Electrophoresis **23**, 1973 (2002).
[9] Y. Terashima, H. Ozaki, and M. Sekine, Water Res. **20**, 537 (1986).
[10] J. H. P. Watson, J. Appl. Phys. **44**, 4209 (1973).
[11] M. Franzreb and W. H. Hoell, IEEE Trans. Appl. Supercond. **10**, 923 (2000).
[12] S. Miltenyi, W. Muller, W. Weichel, and A. Radbruch, Cytometry **11**, 231 (1990).
[13] C. Alexiou, R. J. Schmid, R. Jurgons, M. Kremer, G. Wanner, C. Bergemann, E. Huenges, T. Nawroth, W. Arnold, and F. G. Parak, Eur. Biophys. J. **35**, 446 (2006).
[14] S. Sanchez, A. A. Solovev, S. M. Harazim, and O. G. Schmidt, J. Am. Chem. Soc. **133**, 701 (2011).
[15] T. B. Jones, Cambridge University Press, (1995).
[16] S. Rudge, C. Peterson, C. Vessely, J. Koda, S. Stevens, and L. Catterall, J. Control. Release **74**, 335 (2001).
[17] A. D. Grief and G. Richardson, J. Magn. Magn. Mater. **293**, 455 (2005).
[18] W. Peukert, H. C. C. Schwarzer, and F. Stenger, Chem. Eng. Process. Process Intensif. **44**, 245 (2005).
[19] N. C. L. Hess, D. J. Carlson, J. D. Inder, E. Jesulola, J. R. Mcfarlane, and N. A. Smart, Physiol. Res. **65**, 461 (2016).
[20] R. Werner and B. Wolf-Jürgen, Non-Dest. Test. in Civ. Eng., Germany (2003).